www.vbripress.com, www.amlett.com, DOI: 10.5185/amlett.2011.4252 Published online by the VBRI press in 2012

Electrical properties of complex tungsten bronze ferroelectrics; $Na_2Pb_2R_2W_2Ti_4V_4O_{30}$ (R = Gd, Eu)

Piyush R. Das[1*], B. Pati[2], B.C. Sutar[3], R.N.P. Choudhury[1]

[1]*Department of Physics, Institute of Technical Education and Research, SOA University, BBSR, India*
[2]*Department of Physics, Jupiter Science College, BBSR, India*
[3]*Department of Physics, KMBB College of Engineering and Technology, BBSR, India*

[*]Corresponding author. Tel: (+91) 9438047597; E-mail: prdas63@gmail.com, prdas@iter.ac.in

Received: 16 April 2011, Revised: 26 July 2011 and Accepted: 27 July 2011

ABSTRACT

Complex impedance analysis of new tungsten bronze ferroelectric vanadates, $Na_2Pb_2R_2W_2Ti_4V_4O_{30}$ (R = Gd, Eu), was carried out on samples prepared relatively at low temperature using a mixed-oxide technique. The formation of the materials under the reported conditions has been confirmed by an X-ray diffraction technique. A preliminary structural analysis exhibits orthorhombic crystal structure of the materials at room temperature. The electrical properties of the materials have been studied using ac impedance spectroscopy technique. Detailed studies of impedance and related parameters exhibit that the electrical properties of the materials are strongly dependent on temperature, and bear a good correlation with their microstructures. The temperature dependence of electrical relaxation phenomenon in the materials has been observed. The bulk resistance, evaluated from complex impedance spectra, is found to decrease with rise in temperature, exhibiting a typical negative temperature co-efficient of resistance (NTCR) – type behavior similar to that of semiconductors. A small contribution of grain boundary effect was also observed. The complex electric modulus analysis indicates the possibility of hopping conduction mechanism in the system with non-exponential type of conductivity relaxation. The ac conductivity spectra exhibit a typical signature of an ionic conducting system, and are found to obey Jonscher's universal power law.

Keywords: Electronic material; ceramics; impedance analysis; bulk resistance; electric modulus analysis.

P.R. Das is a postgraduate (1987) in Physics from Ravenshaw college, Cuttack. He did his PhD in Physics (Condense Matter) from IIT Kharagpur in 2008. He is presently working as Associate Professor in the Department of Physics, Institute of Technical Education & Research (Siksha O Anusandhan University), Bhubaneswar, Orissa. His major field of research is in the area of multiferroics/ferroelectric materials. He is presently guiding several research students for PhD degree.

R.N.P. Choudhary has actively been engaged in teaching and research for last 40 years at the institutes of national and international reputes such as IIT and NIT. He is one of the pioneer researchers and contributors in the field of ferroelectrics and related materials in India and abroad. He has guided more than four dozens of PhD students and published more than 500 research papers in international/national journals.

B.C. Sutar did his Postgraduate in physics from Sambalpur Univversity. He is continuing his PhD work in Physics (Condense Matter). He is presently working as Assistant Professor in the Department Of Physics, KMBB College of Eng & Technology,Bhubaneswar, Orissa. His major field of research is in the area of multiferroics/ferroelectric materials.

Introduction

Since the discovery of ferroelectric properties in $BaTiO_3$ of perovskite structural family of ABO_3 type (A=mono-divalent and B=tri-hexavalent ions), a large number of oxides of different structural family have been investigated in the past in search of new and promising materials for industrial applications. It was found that some of the oxides with distorted perovskite structure have complex but stable structure at room temperature with many interesting properties useful for devices. Out of them some materials with tungsten bronze (TB) structure have been found more favourable for high dielectric constant [**1**], electro optic [**2**], pyroelectric [**3**], piezoelectric [**4**], nonlinear optic [**5**], acousto-optic [**6**], photo-refractive [**7**] etc. devices. The TB structure (derived from perovskite ABO_3 type) consists of a complex array of distorted BO_6 octahedral sharing corners in such a way that three different types of interstices (A, B and C) are available for cation substitutions in a general formula $(A_1)_2$ $(A_2)_4$ (C_4) $(B_1)_2$ $(B_2)_8$ O_{30}. In this structure mono or divalent cations can be accommodated at the A-sites (A_1 and A_2), tri or pentavalent cations at octahedral sites (B_1 and B_2) [**8**] and C-site is generally occupied by small ions or empty. It is expected that the substitutions of varieties of cations at the A and B sites change the crystal

structure and physical properties of materials significantly due to their different atomic/ionic size and charge distribution [**9**]. Most of the TB structure belongs to tetragonal or orthorhombic structure with small distortion of multiple perovskites. Some tungsten bronze ferroelectric ceramics are found to be stable at room temperature with diffuse phase transition and relaxor behavior. Also, structural flexibility and chemical versatility of these materials make them more suitable for device applications. Detailed literature survey on the compounds of the TB ferroelectrics reveals that lots of works have been carried out on simple and/or complex niobates and tantalates [**10-18**] in the form of single crystal, ceramics or thin film. In view of the importance of the materials for understanding and applications we have already carried out extensive studies on variety of compounds of this TB structural family. Synthesis, basic crystal structure, ferroelectric and related properties of some complex vanadates such as Na_2 Pb_2 Gd_2 W_2 Ti_4 V_4 O_{30} and Na_2 Pb_2 Eu_2 W_2 Ti_4 V_4 O_{30} [**19**] in the form of ceramics have already been reported by us. Recently structural and electrical properties of Ca modified $Ba_5NdTi_3Nb_7O_{30}$ have been reported by Ganguly et.al [**20**]. Dielectric and pyroelectric properties of $Ba_5SmTi_3Nb_7O_{30}$ have also been reported by them later [**21**]. More recently ferroelectric and related properties of nanocrystalline $Ba_5SmTi_3Nb_7O_{30}$ have been reported by them [**22**].

As it is well known, complex impedance spectroscopic technique is found to be an important and promising non-destructive method for electrical characterization of ferroelectric ceramics. Therefore, we have used complex impedance spectroscopy (CIS) technique to study the electrical processes of $Na_2Pb_2R_2W_2Ti_4V_4O_{30}$ (R= Gd, Eu) as a function of frequency at different temperature which is reported here.

Experimental

Materials preparation

The polycrystalline samples of new complex TB structure compounds, $Na_2Pb_2Gd_2W_2Ti_4V_4O_{30}$ (NPGWTV) and $Na_2Pb_2Eu_2W_2Ti_4V_4O_{30}$ (NPEWTV) were prepared by a standard solid-state reaction (mixed-oxide) method and reported elsewhere [**19**]. An appropriate amount (stoichiometric ratio) of high-purity (AR grade) precursors; Na_2CO_3 (99%, M/s s.d. fine chem. Ltd.), PbO (99.9%, E. Merck India Ltd.), Gd_2O_3, Eu_2O_3 (99.9%, M/s Indian Rare Earth Ltd.), TiO_2 (99%, M/s LOBA Chemie Pvt. Ltd., India), WO_3, V_2O_5 (99.9%, M/s LOBA Chemie Pvt. Ltd., India) was mixed first mechanically in an agate-mortar and pestle for an hour followed by wet grinding (in methanol) for another hour to achieve homogeneous mixture of the constituents. The mixture so obtained was first fired at a temperature of 650^0C for 6 h in air atmosphere. The firing/calcination was repeated (twice) under similar conditions in order to get the reaction of precursor materials completed. The formation of the compounds was checked by preliminary X-ray structural analysis. The calcined powder of the compounds was cold pressed into cylindrical pellets (10 mm diameter and 1-2 mm thickness) with the help of polyvinyl alcohol (PVA) as the binder. An isostatic pressure of 5×10^6 N/m^2 was applied for pelletization. The pellets were then sintered at an optimised temperature (675 ^{0}C) and time (4h). The sintered pellets were then polished to make their faces smooth and parallel. It was then coated with conductive silver paint followed by slow drying for electrical measurements.

Material characteristics

The preliminary structural analysis of the compounds was carried out by X-ray diffraction (XRD) data/pattern. The XRD pattern of the materials was recorded at room temperature using a X-ray powder diffractometer (Rigaku Miniflex) with CuK_α radiation ($\lambda = 1.5405A^0$) in a wide range of Bragg angle θ ($20^0 \le 2\theta \le 80^0$) at a scanning rate of 3^0/min for the purpose. The microstructures of sintered pellets of NPGWTV and NPEWTV were recorded using scanning electron microscope (SEM JEOL JSM – 5800). The impedance and related parameters were measured using a computer-controlled impedance analyser/LCR meter (HIOKI LCR Hi Tester, Model: 3532) as a function temperature over a wide range of frequencies (100 Hz – 1 MHz) and temperatures (30–500 ^{0}C). A chromel - alumel thermo-couple and a digital milli-voltmeter (AGRONIC – 161) were used to measure temperatures. An input ac signal of small voltage amplitude (~10 mV) was applied across the sample cell followed by thermal stabilization for 2h prior to the measurements.

Results and discussion

Samples preparation

The formation of single phase desired compounds (NPGWTV and NPEWTV) at room temperature was confirmed based on preliminary structural analysis using X-ray diffraction (XRD) technique. Detailed studies of XRD pattern of the two compounds and their lattice parameters have been reported earlier [**19**]. The calculated values of crystallite size (average) P of NPGWTV and NPEWTV using Scherrer equation: $P = k\lambda/(\beta_{1/2}\text{Cos}\theta)$, where $k = 0.89$, $\lambda = 1.5405$Å and $\beta_{1/2}$ = broadening of peak, were found to be 17nm and 16nm respectively. As the powder samples were used to get XRD pattern, contributions of strain and other effects in the broadening and crystallite size calculation have been ignored.

Impedance spectrum analysis

Impedance spectroscopy (IS) is the most reliable technique to study the electrical properties and process of the materials. The IS technique is based on analyzing the ac response of a system to a sinusoidal perturbation, and subsequent calculation of impedance and related parameters as a function of frequency of the perturbation. Each parameter can be used to highlight a particular aspect of the materials. A parallel resistance and capacitance circuit corresponding to equivalent to the individual component of the materials (i.e., bulk and grain boundary) represents a semicircle. Impedance data of materials (i.e., capacitive and resistive components), represented in the

Nyquist plot, lead to a succession of semicircle. The electrical properties are often presented in terms of impedance (Z) [**23-27**], permittivity (ε) [**26**] and electrical modulus (M) [**30-32**]. The frequency dependence of dielectric properties of the materials is normally described in terms of complex dielectric constant (ε^*), complex impedance (Z*), electric modulus (M*) and dielectric loss ($\tan\delta$) and are related to each other as

$$Z^* = Z' - jZ'' = R_s - \frac{j}{\omega c_s}, \varepsilon^* = \varepsilon' - j\varepsilon'',$$

$$M^* = M' + jM'' = j\omega Co Z^* \omega, \ \tan\delta = \frac{\varepsilon''}{\varepsilon'} = \frac{Z'}{Z''} = \frac{M''}{M'}$$

where ω is the angular frequency, ε_0 is the permittivity in free space, Rs and Cs are resistance and capacitance in series respectively. As the above expressions offer a wide scope for graphical representation, they can be used to calculate complex impedance of the electrode/ceramic/electrode capacitor (demonstrated as the sum of the single RC circuit with parallel combination) as per the relation:

$$Z^*(T) = Z_0(T)\int \frac{Y(\tau, T)\,d(\tau)}{1 + j\omega\tau}$$

Separating the real and imaginary part of the above equation, they can be written as

$$Z'(\omega, T) = Z_0(T)\int \frac{Y(\tau, T)\,d(\tau)}{1+\omega^2\tau^2}$$

$$Z''(\omega, T) = Z_0(T)\int \frac{(\omega\tau)^* Y(\tau, T)\,d(\tau)}{1+\omega^2\tau^2}$$

Here, $\tau = RC$ represents the relaxation time, T= time period and Y (τ , T) = distribution function of relaxation time. The variation of imaginary part of complex impedance $Z''(\omega, T)$ provides information about the distribution function Y (τ , T).

Fig. 1 shows the variation of real part of impedance (Z' , i.e., bulk resistance) with frequency at different temperatures. The values of Z' decrease with rise in frequency and temperature. The magnitude of Z' decreases on increasing temperature in the low- frequency range which merges in the high-frequency region irrespective of temperature. This nature may be due to the release of space charge [**33**]. The reduction in barrier properties of the materials with rise in temperature may be a responsible factor for enhancement of a.c. conductivity of the materials at higher frequencies [**30-31**]. Further, in the low frequency region, there is a decrease in magnitude of Z' with rise in temperature showing negative temperature coefficient of resistance (NTCR) behavior. This behaviour is changed drastically in the high frequency region showing complete merger of Z' plot above a certain fixed frequency. A particular frequency at which Z' becomes independent of frequency was observed to shift towards the higher frequency side (with rise in temperature). The shift in Z' plateau indicates the existence of frequency relaxation process in the material. The curves display single relaxation process and indicate the increase in a.c. conductivity with increase in temperature and frequency [**28**].

Fig. 2 shows the variation of imaginary part of impedance (Z'') with frequency (i.e., loss spectrum) at different temperatures. The loss spectrum of the materials can be characterized by few important features such as, (i) a monotonous decrease in Z'' in the low temperature region, (ii) appearance of peaks in the loss spectrum at high temperatures, (iii) significant peak broadening with increase in temperature, and (iv) existence of symmetric peak broadening. The absence of peaks upto a temperature of 275 ^{0}C in the loss spectrum suggests the absence of current dissipation in this low temperature region. The pattern shows peaks at a particular frequency which describes the type and strength of electrical relaxation phenomenon in the materials [**28**]. The value of Z'' reaches a maximum peak (Z''_{max}) above 325^0 C. It is expected that low temperature peaks (< 350^{0}C), was beyond the range of frequency used. The Z''_{max} shifts to higher frequency side on increasing temperature indicating increase of tangent loss in the samples. A significant increase in the broadening of the peaks with increase in temperature suggests the existence of a temperature dependence of electrical relaxation phenomenon in the materials. The relaxation process may be due to the presence of electrons / immobile species at low temperatures and defects / vacancies at higher temperatures. The asymmetric broadening of the peaks suggests a spread of relaxation time with two equilibrium positions. The peak heights are proportional to bulk resistance (R_b), and can be estimated and explained by the equation, $Z''[= R_b\{\omega\tau/(1+\omega^2\tau^2)\}]$ in Z'' versus frequency plots. Further, the magnitude of Z'' decreases gradually with a shift in peak frequency towards high frequency side, and it finally merges in the high frequency region. This is an indication of the accumulation of space charge in the materials.

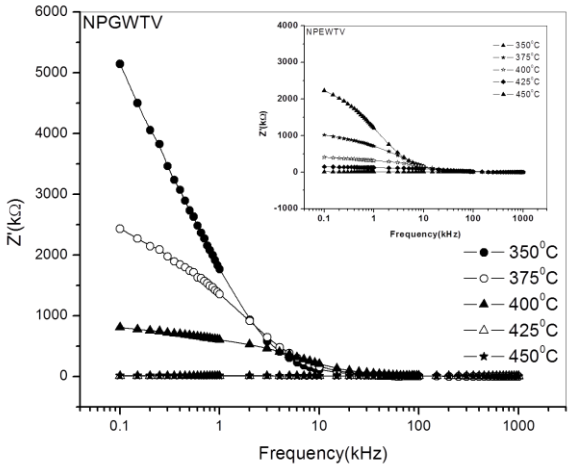

Fig. 1. Variation of real part of impedance (Z') with frequency of NPGWTV and NPEWTV (inset).

Fig. 3 shows complex impedance spectrum (Nyquist plot) of NPEWTV and NPGWTV measured at different temperatures over a wide range of frequency range (100 Hz – 1MHz). The effect of temperature on impedance

characteristics of the materials becomes clearly visible in the figure. The impedance property of the materials is characterized by the appearance of semicircular arcs whose pattern of evolution changes with change in temperature. The extent of intercept on the real axis and its number in the spectrum provide very important information on electrical behaviour of the materials under investigation. Such pattern provides information on the kind of electrical processes occurring within the materials and their correlation with microstructure when modeled in terms of an equivalent electrical circuit. The semicircular arcs of the impedance pattern can mainly be attributed to a parallel combination of resistance and capacitance. As temperature increases, the arc progressively becomes semicircular with a shift of the centre towards origin of the complex plane plot. With further increase in temperature, the slope of the line decreases, and bend towards Z' - axis (above 350^0C), and thus a semicircle could be traced indicating the increase in conductivity of the sample [**30-31**]. The presence of semicircular arcs for temperatures upto 425^0C suggests that the electrical processes in the materials arise basically due to the contribution from bulk material (grain interior), and can be modeled as an equivalent electrical circuit comprising of a parallel combination of bulk resistance (R_b) and bulk capacitance (C_b) [**32**]. The electrical process at these temperatures may be considered due to intra-grain phenomenon. However, a tendency to form a small semicircle is seen in the Z' - Z'' plots at high temperatures indicating very small contributions of grain boundary in the materials. Thus detailed analysis of second semicircles has been ignored here. The value of R_b and C_b at different temperatures can be obtained from impedance spectrum. It can be seen that the values of R_b and C_b decrease with rise in temperature. The decrease in R_b with the rise in temperature indicates the NTCR behaviour of NPEWTV and NPGWTV, which was also observed in Z' versus frequency plot. The relaxation time (τ) was estimated from the maxima of the semicircle (due to bulk effect) of the complex impedance plots.

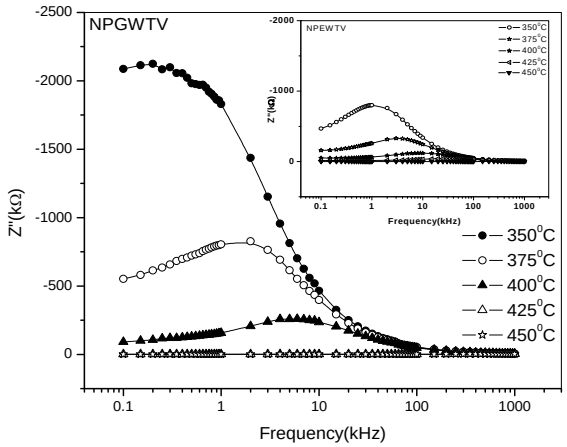

Fig. 2. Variation of imaginary part of impedance (Z'') with frequency of NPGWTV and NPEWTV (inset).

Complex electric modulus analysis

The complex modulus formalism is very convenient tool to interpret the dynamical aspects of electrical transport phenomena. This technique also provides an insight into the electrical processes using the following relations of electrical modulus.

$$M' = A\left[\frac{(\omega RC)^2}{1+(\omega RC)^2}\right] = A\left[\frac{\omega^2\tau^2}{1+\omega^2\tau^2}\right];$$

$$M'' = A\left[\frac{\omega RC}{1+(\omega RC)^2}\right] = A\left[\frac{\omega\tau}{1+\omega^2\tau^2}\right] \text{ Where } A = \frac{C_0}{C}$$

Using the above modulus formalism the inhomogeneous nature of polycrystalline ceramics with bulk and grain boundary effects can easily be probed, which cannot be distinguished from complex impedance plots. The other major advantage of the electric modulus formalism is to suppress the electrode effect.

The complex electric modulus is usually calculated from the impedance data using the following relations: $M^* = M' + jM'' = \frac{1}{\varepsilon^*} = j\omega\varepsilon_0 Z^*$ where, $M' = \omega C_0 Z''$ and $M'' = \omega C_0 Z'$, $\omega = 2\pi f$ = angular frequency, C_0 = geometrical capacitance $= \frac{\varepsilon_0 A}{t}$, ε_0 = permittivity of free space, A = area of electrode surface, t = thickness.

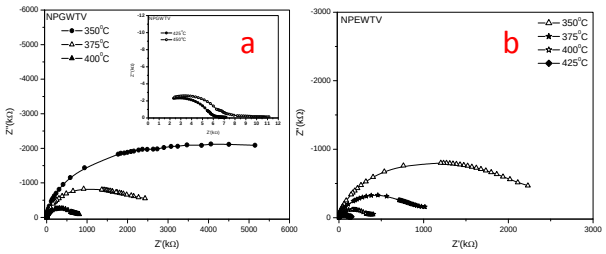

Fig. 3. (a) Nyquist (Z'- Z'') plot of the compound NPGWTV at different temperature. (b)Nyquist (Z'- Z'') plot of the compound NPEWTV at different temperatures.

Fig. 4 shows the variation of M' as a function of frequency for NPGWTV and NPEWTV at selected temperatures. These figures exhibit that M' approaches to zero in the low frequency region, and a continuous dispersion on increasing frequency, with a tendency to saturate at a maximum asymptotic value (i.e., M_∞) in the high frequency region at all the temperatures. Such observation may possibly be related to a lack of a restoring force governing the mobility of the charge carriers under the action of an induced electric field. This behaviour supports the short range mobility of charge carrier.

Fig. 5 shows the variation of M'' with frequency for NPGWTV and NPEWTV at selected temperatures. It is clear from the figures that the modulus spectrum is broader and the peaks are asymmetric. The peaks shift towards higher frequency side on increasing temperature of the

samples. This behaviour suggests that the spectral intensity of the dielectric relaxation is activated thermally in which hopping process of charge carriers and small polarons dominate intrinsically. Both the electric modulus and the impedance formalism plots produce peaks, which are broader as compared to that predicted by Debye for relaxation phenomenon, and are significantly asymmetric. The relaxation time (τ) associated with each peak is determined from the frequency at which M''_{max} occurs. At the maxima of M'' the equation $\tau = \frac{1}{2\pi f}$ holds good. The magnitude of the peak increases on increasing temperature. The broad envelope of electrical relaxation can be assigned to relaxation occurring within the bulk of the materials [**27-28**].

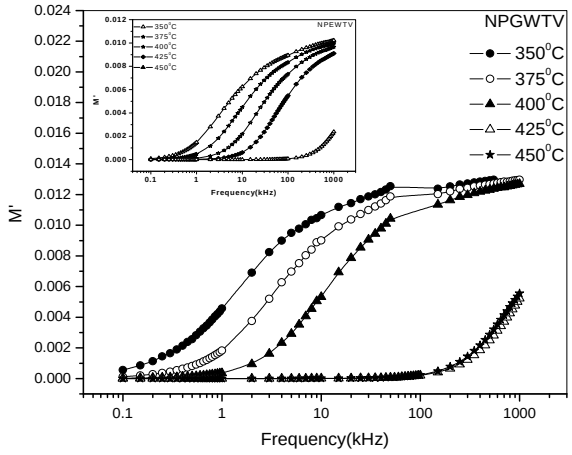

Fig. 4. Variation of real part of modulus (M') with frequency of NPGWTV and NPEWTV (inset)

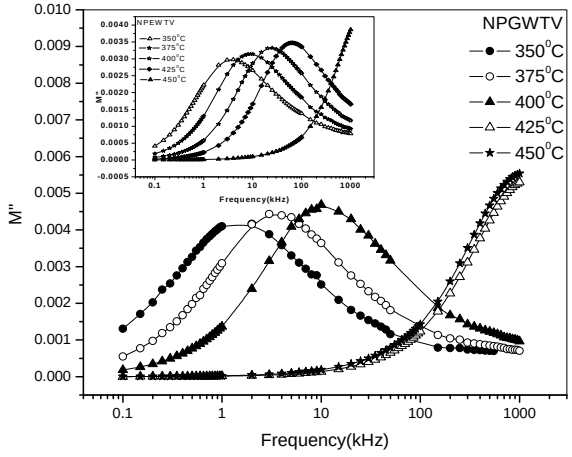

Fig. 5. Variation of imaginary part of modulus (M'') with frequency of NPGWTV and NPEWTV (inset)

Fig. 6 shows the complex modulus spectrum i.e., (M' vs M'') of NPGWTV and NPEWTV at selected temperatures. The asymmetric semicircular arc observed earlier is now confirmed from this method and appears to overlap at all the temperatures. This may be due to the presence of electrical relaxation phenomena in the materials. The curves don't form semicircles as required for the ideal Debye model. Rather they possess the shape of deformed arcs with their centres positioned below the x-axis. This indicates the spread of relaxation with different mean time constants, and hence non-Debye type of relaxation in the material is confirmed. However the single semicircular arc confirms the formation of single- phase compounds, which is also evident from XRD studies. The modulus plane shows a single semicircle and its intercept on the real axis is the total capacitance contributed by the grain and grain boundaries. Further, it is confirmed from our M'' vs. frequency plot that the grain boundary effect is negligibly small or zero, and does not affect the relaxation process much. However, there is a marked change in the shape and size of modulus spectrum with rise in temperature suggesting a change in the capacitance value of the material with temperature.

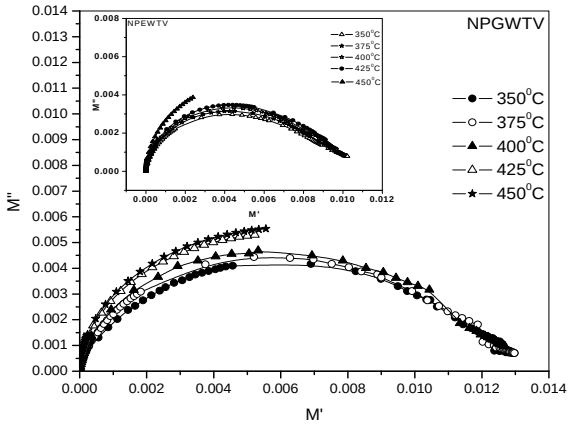

Fig. 6. Complex modulus spectrum of NPGWTV and NPEWTV at different temperatures (inset)

A.C. conductivity analysis

The frequency dependence of ac conductivity ($\sigma(\omega)$) at various temperatures is shown in **Fig. 7**. In the low temperature region the conductivity increases with increase in frequency which is a characteristic of ω^n (n = exponential). At higher temperatures and low frequencies, conductivity shows a flat response while it has ω^n dependence at high frequencies. The phenomenon of the conductivity dispersion in solids is generally analysed using Jonscher's power law; $\sigma(\omega) = \sigma_{dc} + A\omega^n$, where σ_{dc} is the dc conductivity at a particular temperature, A is temperature dependent constant and n is temperature dependent exponent in the range of $0 \leq n \leq 1$. The n represents the degree of interaction between mobile ions with the lattices around them, and A determines the strength of polarisability. The materials obey universal power law, and are confined by a typical fit of the above equation to the experimental data (**Fig. 8**). The estimated value of n is 0.6458 for NPEWTV at a temperature of 300 ^oC and 0.47 for NPGWTV at a temperature of 350 ^oC. According to Jonscher [**34**], the origin of frequency

dependence of conductivity lies in the relaxation phenomenon arising due to mobile charge carriers. The low frequency dispersion attributes to the ac conductivity whereas the frequency independent plateau region of the conductivity pattern corresponds to dc conductivity of the material. The temperature at which grain resistance dominates over grain boundary resistance is marked by a change in slope of ac conductivity with frequency. The frequency at which the change of slope takes place is known as the hoping frequency. It corresponds to polaron hopping of charged species. The hopping frequency shifts to higher frequency side on increasing temperature. The charged species that have been accumulated at the grain boundaries have sufficient energy to jump over the barrier on increasing temperature. It is clear from **Fig. 7** that at high temperatures and low frequencies, the curves tend to merge with a constant slope. This frequency independent behaviour is attributed to the contribution from dc conduction.

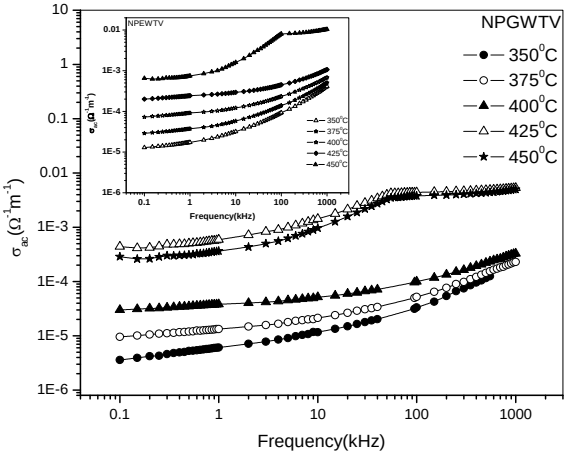

Fig. 7. Variation of ac conductivity σ (ω) with frequency of NPGWTV and NPEWTV (inset).

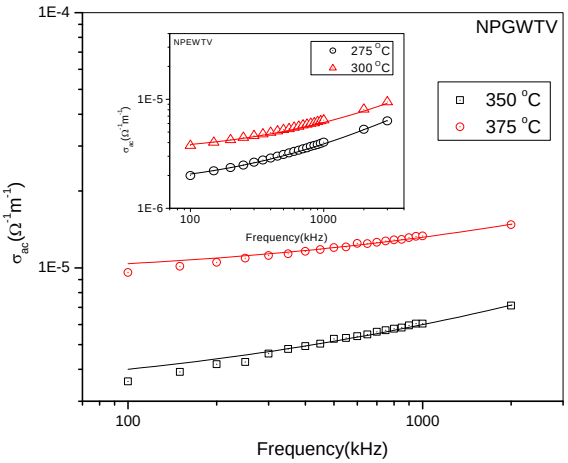

Fig. 8. ac fitting curve for NPGWTV and NPEWTV at different temperatures (inset)

Conclusion

The present work represents the results of our investigation on the electrical properties of new tungsten bronze ferroelectric vanadates $Na_2Pb_2R_2W_2Ti_4V_4O_{30}$ (R = Gd, Eu) using complex impedance spectroscopy (CIS). The experimental results on electrical properties indicate that the materials exhibit (i) electrical transport (conduction) due to bulk material, (ii) negative temperature coefficient (NTCR) – type behavior, and (iii) temperature dependent relaxation phenomenon.

Complex impedance analysis suggests the dielectric relaxation in the materials is of polydispersive non-Debye type. The complex electric modulus analysis has confirmed the single-phase behaviour of the material in agreement with the information obtained from XRD pattern. Electrical modulus analysis indicated non-exponential type conductivity relaxation in the material. The frequency dependence of ac conductivity obeys Jonscher's universal power law.

Reference

1. Zhu, X.L.; Chen, X.M.; Liu, X.Q.; Yuan, Y. *J. Mater. Res.* **2006**, *21*, 1787. **DOI:** 10.1557/jmr.2006.0201
2. Huang, C.; Bhalla, A.S.; Guoa, R. *Appl. Phys. Lett.* **2005**, *86*, 211907. **DOI:** 10.1063/1.1937997
3. Rao, K.S.; Nath, N.V. *Ferroelectrics* **2005**, *325*, 15. **DOI:** 10.1080/00150190500326605
4. Jiang, W.; Cao, W.; Yi, X.; Chen, H. *J. Appl. Phys.* **2005**, *97*, 094106. **DOI:** 10.1063/1.1881777
5. Ramirez, M.O.; Jaque, D.; Bausa, L.E.; Garcia, J.S.; Kaminskii, A.A. *Phys. Rev. Lett.* **2005**, *95*, 26740. **DOI:** 10.1103/PhysRevLett.95.267401
6. Venturini, E.L.; Spencer, E.G.; Ballman, A.A. *J. Appl. Phys.* **1969**, *40*, 1622. **DOI:** 10.1063/1.1657822
7. Lee, M.; Feigelson, R.S. *Opt. Mater.* **2003**, *21*, 759. **DOI:** 10.1016/S0925-3467(02)00096-4
8. Jamieson, P.B.; Abrahams, S.C.; Bernstein, L. J. Chem. Phys. **1968**, *48*, 5048. **DOI:** 10.1063/1.1668177
9. Neurgaonkar, R.R.; Nelson, J.G.; Oliver, J.R. Mater. Res. Bull. **1990**, *25*, 959. **DOI:** 10.1016/0025-5408(90)90002-J
10. Raju, M.R.; Choudhary, R.N.P. *Mater. Chem. Phys.* **2006**, *99*, 135. **DOI:** 10.1016/j.matchemphys.2005.09.084
11. Chen, W.; Kinemuchi, Y.; Watari, K.; Tamura, T.; Miwa, K. *J. Am. Ceram. Soc.* **2006**, *89*, 381. **DOI:** 10.1111/j.1551-2916.2005.00694.x
12. Ko, J.H.; Kojima, S.; Lushnikov, S.G.; Katiyar, R.S.; Kim, T.H.; Ro, J.H. *J. Appl. Phys.* **2002**, *92*, 1536. **DOI:** 10.1063/1.1491995
13. Singh, A.K.; Choudhary, R.N.P. *Ferroelectrics* **2005**, *325*, 7. **DOI:** 10.1080/00150190500326522
14. Kim, M.S.; Lee, J.H.; Kim, J.J.; Lee, H.Y.; Cho, S.H. *J. Solid State Electrochem.* **2006**, *10*, 18. **DOI:** 10.1007/s10008-005-0647-9
15. Fang, L.; Zhang, H.; Huang, T.H.; Yuan, R.Z.; Liu, H.X. *J. Mater. Sci.* **2005**, *40*, 533. **DOI:** 10.1007/s10853-005-6122-2
16. Behera, B.; Nayak, P.; Choudhary, R.N.P. *Mater. Chem. Phys.* **2006**, *100*, 138. **DOI:** 10.1016/j.matchemphys.2005.12.022
17. Das, P.R.; Choudhary, R.N.P.; Samantray, B.K. Mater. Chem. Phys. 2007, 101, 228. **DOI:** 10.1016/j.matchemphys.2006.04.005
18. Das, P.R.; Choudhary, R.N.P.; Samantray, B.K. J. Alloys Comp. **2008**, *448*, 32. **DOI:** 10.1016/j.jallcom.2006.10.090

19. Das, P.R.; Choudhary, R.N.P.; Samantray, B.K. *J. Phys. Chem. Solids* **2007**, *68*, 516. **DOI:**10.1016/j.jpcs.2007.01.015
20. Ganguli, P.; Jha, A.K. *Int. Ferroelectrics* **2010**, *115*, 149. **DOI:** 10.1080/10584587.2010.488566
21. Ganguli, P.; Devi, S.; Jha, A.K. *Ferroelectrics* **2009**, *381*, 111. **DOI:** 10.1080/00150190902869772
22. Ganguli, P.; Jha, A.K. *J. Am. Ceram. Soc.* **2011**, *94[6]*, 1725. **DOI:** 10.1111/j.1551-2916.2010.04321.x
23. Sen, S.; Choudhary, R.N.P. *Mater. Chem. Phys.* **2004**, *87*, 256. **DOI:** 10.1016/j.matchemphys.2004.03.005
24. Brahma, S.; Choudhary, R.N.P.; Thakur, A.K. *Physica B* **2005**, *355*, 188. **DOI:** 10.1016/j.physb.2004.10.091
25. J.R. Macdonald, Impedance Spectroscopy Emphasizing Solid Materials and Systems, Wiley, New York, *Chap 4*, **1987**.
26. Suchanicz, J. Mater. Sci. Eng. B 1998, 55, 114. **DOI:** 10.1016/S0921-5107(98)00188-3
27. Suman, C.K.; Prasad K.; Choudhary, R.N.P. *J. Mater. Sci.* **2006**, *41*, 369. **DOI:** 10.1007/s10853-005-2620-5
28. Chatterjee, S.; Mahapatra, P.K.; Choudhary, R.N.P.; Thakur, A.K. *Phys. Stat. Sol.(a)* **2004**, *201*, 588. **DOI:** 10.1002/pssa.200306741
29. Borsa, F.; Torgeson, D.R.; Martin, S.W.; Patel, H.K. *Phy. Rev. B* **1992**, *46*, 795. **DOI:** 10.1103/PhysRevB.46.795
30. Provenzano, V.; Boesch, L.P.; Volterra, V.; Moynihan, C.T.; Macedo, P.B. *J. Am. Ceram. Soc.***1972**, *55*, 492. **DOI:** 10.1111/j.1151-2916.1972.tb13413.x
31. Jain, H.; Hsieh, C.H. *J. Non-Cryst. Solids* **1994**, *172*, 1408. **DOI:** 10.1016/0022-3093(94)90669-6
32. Hodge, I.M.; Ingram, M.D; West, A.R. *J. Elect. Chem.* **1975**, *58*, 429.
33. Macedo, P.B/; Moynihan, C.T.; Bose, R. *Phys. Chem.* **1972**, *13*, 171. **DOI:** 10.1021/j100599a016
34. Joncher, A.K. *Phys. Thin films* **1980**, *11*, 232.